Med Chem Res
DOI 10.1007/s00044-017-1838-5

MEDICINAL CHEMISTRY RESEARCH

ORIGINAL RESEARCH

Synthesis, spectral, biological activity, and crystal structure evaluation of novel pyrazoline derivatives having sulfonamide moiety

Rajitha Sadashiva[1] · Damodara Naral[2] · Jyothi Kudva[3] · Naveen Shivalingegowda[4] · Neratur Krishnappagowda Lokanath[5] · Kudigana Jayaprakash Pampa[6]

Received: 2 February 2016 / Accepted: 1 March 2017

Abstract In the present study, synthesis and characterization of pyrazoline derivatives integrated with sulfonamide scaffold have been performed. The characterization of the molecules was done by elemental analysis, ultraviolet–visible, infrared, nuclear magnetic resonance (NMR), and mass spectra. Crystal structure of compounds **2e** and **2g** were determined by single crystal X-ray diffraction. In the compounds **2e** and **2g**, the intra molecular hydrogen bonds N15--H15…O13 and N14--H14…N1 were closed to form a *S(6)* ring motif, whereas the N14--H14…O17 hydrogen bond links, pairs of molecules related by inversion, forming the familiar $R^2_2(10)$ ring motif. The Hirshfeld surface analysis comprising of the d_{norm} surface plots, electrostatic potentials and two-dimensional fingerprint plots were generated in order to give visual confirmation of the intermolecular interactions. The molecules were screened for their in vitro antitubercular and antimicrobial activity. The molecules **2n** and **2m** have shown high potent against *M. tuberculosis* and most of the molecules have shown good potential against different bacteria and fungi.

Keywords *Mycobacterium tuberculosis* · Antimicrobial · Pyrazolines · Sulfonamides · X-ray diffraction analysis

Introduction

Tuberculosis (TB) is a widespread infectious disease caused by various strains of mycobacterial, which is usually *M. tuberculosis*. It remains one of the world's deadliest communicable diseases. TB was slowly declining each year and it was estimated that 37 million lives were saved between the year 2000 and 2013 through effective diagnosis and treatment (WHO Global Tuberculosis Report 2014). There were very few antimicrobial agents available that can be used for life-threatening microbial infections. So the development of an effective antimycobacterial drug is an emerging opportunity in the field of drug discovery.

Pyrazolines are well known nitrogen containing five-membered heterocyclic compounds, which possesses a wide range of biological activity. Pyrazoline derivatives are known for their prominent property as drugs like, pyrazofurin (antibiotic), sulfinpyrazone (uricosurgic), and metamizole (antipyretic). Numerous studies demonstrated that, the pyrazoline derivatives exhibit antibacterial (Shaharyar et al. 2006; Ali et al. 2007; Siddiqui et al. 2011), antidepressant (Prasad et al. 2005), anticonvulsant (Batulin 1968; Parmar et al. 1974; Soni et al. 1987), antihypertensive (Turan-Zitouni et al. 2000), antitumor (Bano et al. 2011) activity. Some of the pyrazoline derivatives are reported to

✉ Jyothi Kudva
jyothikudva@gmail.com

1 Sigma-Aldrich Chemical Pvt. Ltd., Bommasandra-Jigani link Road, Bengaluru 560100, India

2 Department of Chemistry, Canara Engineering College, Benjanapadavu, Mangaluru 574219, India

3 Department of Chemistry, St. Joseph Engineering College, Vamanjoor, Mangaluru 575005, India

4 Institution of Excellence, Vijnana Bhavana, University of Mysore, Manasagangotri, Mysuru 570006, India

5 Department of Studies in Physics, University of Mysore, Manasagangotri, Mysuru 570006, India

6 Department of Studies in Microbiology, University of Mysore, Manasagangotri, Mysuru 570006, India

Published online: 15 March 2017

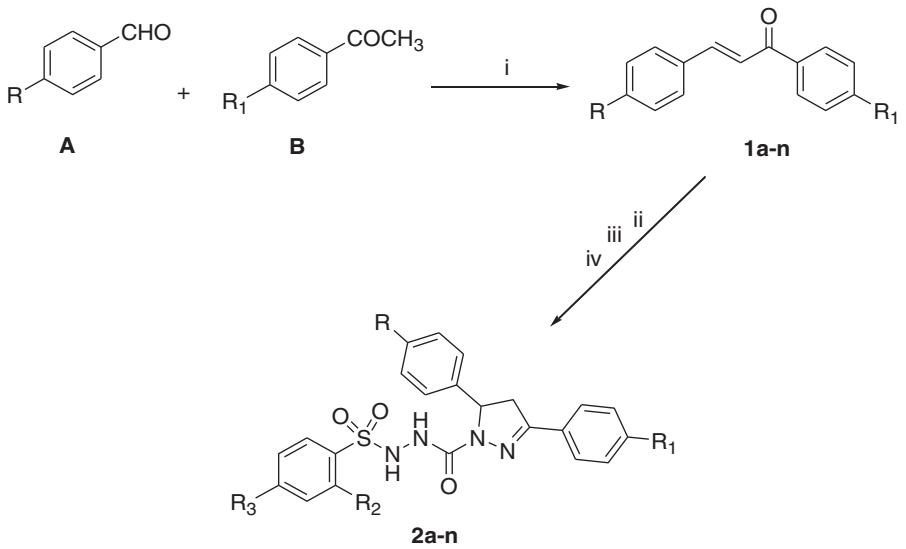

Scheme 1 Synthetic pathway for pyrazoline derivatives integrated with sulfonamide scaffold. Reagents and conditions: (i) Ethanol, KOH, RT, 10 h; (ii) CH3OCONHNH$_2$, methanol, 70 °C, 5 h; (iii) N2H$_4$. H$_2$O, methanol, 80 °C, 8 h; (iv) Fluorosubstituted benzene sulfonyl chloride, CH_2Cl_2, pyridine, 5 °C, 2 h

Compounds	2a	2b	2c	2d	2e	2f	2g	2h	2i	2j	2k	2l	2m	2n
R	H	F	Br	Cl	OCH_3	CH_3	OCH_3	F	H	CH_3	Br	SCH_3	Cl	H
R_1	H	H	H	H	H	H	H	F	H	H	H	H	H	H
R_2	H	H	F	H	H	H	F	H	F	F	H	H	H	H
R_3	F	F	F	F	F	F	F	F	F	F	H	H	H	H

possess anti-inflammatory (Bansal et al. 2001) and anti-diabetic activity (Ahn et al. 2004).

Sulfa drug was the first drug largely employed and systematically used as preventive and chemotherapeutic agent against various diseases (Sammes 1990). The sulfonamide derivatives were reported as orally active endothalins selective antagonists (Kanda et al. 2001), antibacterial (Stokes et al. 2012), antiprotozoal (Chibale et al. 2001), antifungal (Ezabadi et al. 2008), anti-inflammatory (Kennedy and Thorley 1999), nonpeptidic vasopressin receptor antagonists (Gal 2001) and translation initiation inhibitors (Natarajan et al. 2004).

Pyrazoline derivatives integrated with sulfonamide scaffold have the capacity of inhibiting the human carbonic anhydrase isoenzymes in a noncompetitive manner and the inhibition effects of some molecules for isozymes were almost in nanomolar concentration range (Balseven et al. 2013). The pyrazoline and sulfonamide integrated molecules have shown the anticancer and anti-inflammatory (Bashir et al. 2011) capacity and some of the pyrazoline derivatives were discovered as fluorescent probe for detecting glutathione among biological thiols in aqueous media (Wang et al. 2013).

In view of the potential application of pyrazoline and sulfonamide derivatives, synthesis of new series of pyrazolines integrated with sulfonamide scaffold (2a–n) was undertaken. The molecules were structurally characterized by elemental analysis, ultraviolet (UV)– visible (Vis), infrared (IR), nuclear magnetic resonance (NMR), and mass spectra. The antitubercular property was studied against *M. tuberculosis* H37Rv and antimicrobial property was studied against *Staphylococcus aureus* MTCC 96, *Bacillus subtilis* MTCC 441, *Pseudomonas aeruginosa* MTCC 1688, *Escherichia coli* MTCC 443, *Aspergillus fumigatus* ATCC1028, *Aspergillus niger* MTCC 282, *Candida albicans* MTCC 227, and *Aspergillus flavus* ATCC 9643. The detailed single crystal X-ray diffraction study and Hirshfeld surface analysis were carried out for the compounds **2e** and **2g**.

Results and discussion

Chemistry

The synthetic route for target pyrazoline derivatives integrated with sulfonamide scaffold **2a–n** was carried out as outlined in Scheme 1. The substituted chalcones **1a–n** were prepared as per well-known Claisen-Schmidt reaction using *para* substituted arylaldehydes (**A**) and *para* substituted acetophenones (**B**). The *N*-methyl ester substituted pyrazoline ring was constructed by the reaction of suitable chalcone with methyl hydrazine carboxylate in methanol. The corresponding carbohydrazide derivatives of pyrazoline were synthesized by the reaction of *N*-methyl ester substituted pyrazoline derivatives with hydrazine hydrate. The required pyrazoline derivatives integrated with sulfonamide scaffold was obtained by the reaction of fluorosubstituted benzene sulfonyl chloride with pyrazoline carbohydrazide derivatives in the presence of pyridine.

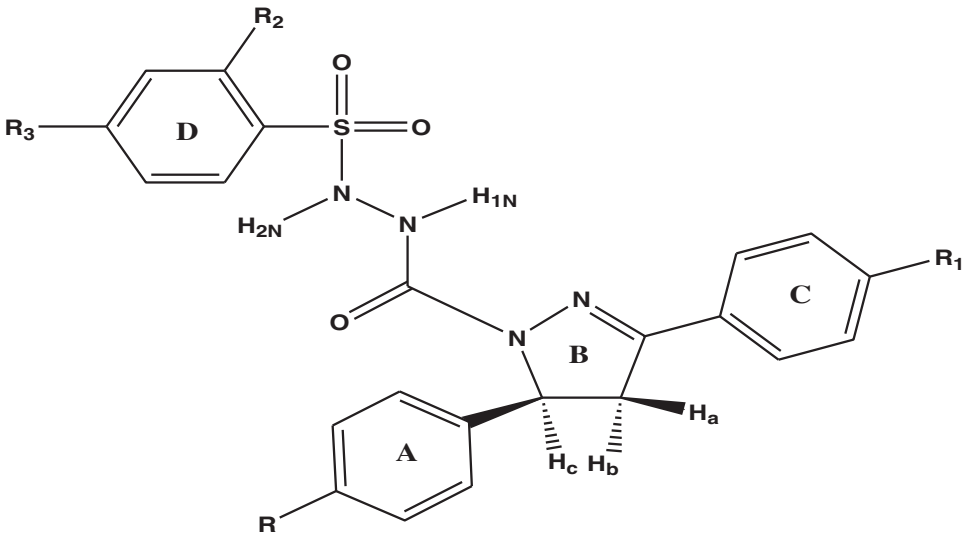

Fig. 1 Labeling of atoms and rings of pyrazoline derivatives integrated with sulfonamide scaffold (**2a–n**)

Spectral analysis

The synthesized molecules **2a–n** exhibit intense absorption band in UV–Vis spectra, which was attributed to the π–π* transition of the conjugated backbone (Sverdlova et al. 1968). The absorption maximum (λ_{max}) was found in the range of 293–298 and 217–223 nm, which was due to absorption of $-SO_2-NH-$ and Ar–N–N=C–Ar groups, respectively (Bhat et al. 2009; Sheat et al. 2011).

Infrared spectra of the synthesized compounds were recorded in the region 4000–400 cm^{-1}. The strong stretching bands in the region 3400–3100 cm^{-1} indicate the presence of N–H group. The asymmetric and symmetric stretching bands of SO_2 group were observed in the region 1340–1150 cm^{-1}, respectively (Stuart 2004). The C=O stretching frequency was obtained in the region of 1650 cm^{-1}. The absorption bands in the region 1583–1618 cm^{-1} indicate the C=N stretching frequency (Stuart 2004).

The NMR spectra of the compounds were recorded in DMSO-d_6. The pyrazoline nucleus has two geminal protons H_a and H_b, which were magnetically non-equivalent due to the presence of chiral proton H_c in the adjacent carbon (Fig. 1). These three pyrazoline protons displayed three doublet of doublets as ABX pattern with varying coupling constant (J) values. The protons H_a and H_b were resonated at δ, 3.00 and 3.60 ppm, respectively. The chiral proton H_c was resonated in the region δ, 5.50–6.00 ppm, which was due to vicinal coupling with adjacent two protons H_a and H_b. This confirms the presence of pyrazoline ring in the compound (Hassner and Michelson 1962). All the aromatic protons were resonated in the region between δ, 7.00 and 8.00 ppm. The two amine protons, H_{2N} and H_{1N} were resonated in the region δ, 9.00–9.90 ppm. In ^{13}C NMR spectra, methylene carbon atom of pyrazoline ring was resonated from δ, 40.3 to 48.5 ppm. The methine and azomethine carbon atom of pyrazoline ring were resonated from δ, 62.3 to 67.9 ppm and δ, 150.1 to 154.0 ppm, respectively. The aromatic carbons were resonated between δ, 105.38 and 166.14 ppm. The mass spectra of all synthesized pyrazoline derivatives **2a–n** were recorded and m/z value of all the compounds has the correlation with the theoretical molecular weight of the compounds. The purity of the compounds was analyzed by elemental analysis.

Biology

Antitubercular studies

The antitubercular potency of the synthesized molecules **2a–n** was screened by micro plate alamar blue assay (MABA). The alamar blue oxidation-reduction dye is a general indicator of cellular growth and/or viability; the blue, non-fluorescent, oxidized form becomes pink and fluorescent upon reduction. The activity was expressed as the minimum inhibitory concentration (MIC) in μg/mL (Table 1).

The MIC value of each compound was depended on the nature of the group present at R, R_1, R_2, and R_3 (Fig. 1). The compound **2n**, which has the neat phenyl ring A, C, and D have shown an excellent potency, which was 7.81-fold more potent than the streptomycin and 3.9-fold more potent than the pyrazinamide and ciprofloxacin. The compound **2m** (R=Cl) has shown MIC 1.6 μg/mL, which was 3.90-fold more potent than the standard drug streptomycin and 1.9-fold more active than the pyrazinamide and ciprofloxacin. The derivatives with neat phenyl ring D, such as

Table 1 Antitubercular and antimicrobial activity data of compound **2a–n** in terms of MIC (μg/mL)

Compounds	MIC (μg/mL)								
	M. tuberculosis	Gram-positive bacteria		Gram-negative bacteria		Fungi			
		S. a[a]	*B. s*[b]	*E. c*[c]	*P. a*[d]	*A. f*[e]	*A. n*[f]	*A. f*[g]	*C. a*[h]
2a	25.0	75.0	50.0	75.0	50.0	–	75.0	50.0	–
2b	50.0	100.0	50.0	25.0	50.0	–	75.0	–	50.0
2c	100.0	150.0	50.0	75.0	75.0	75.0	25.0	50.0	50.0
2d	12.5	125.0	100.0	100.0	50.0	150.0	50.0	100.0	50.0
2e	12.5	75.0	50.0	50.0	50.0	100.0	25.0	100.0	75.0
2f	50.0	75.0	75.0	75.0	50.0	–	50.0	75.0	75.0
2g	6.25	75.0	75.0	50.0	50.0	–	–	25.0	–
2h	100.0	75.0	50.0	100.0	75.0	–	50.0	–	–
2i	12.5	75.0	50.0	75.0	50.0	75.0	50.0	10.0	25.0
2j	50.0	100.0	75.0	75.0	75.0	–	–	50.0	50.0
2k	3.12	–	50.0	–	50.0	50.0	50.0	50.0	–
2l	3.12	–	50.0	–	50.0	–	50.0	75.0	50.0
2m	1.6	75.0	75.0	–	50.0	–	–	50.0	75.0
2n	0.8	75.0	–	–	–	50.0	50.0	50.0	50.0
Pyrazinamide	3.125	–	–	–	–	–	–	–	–
Streptomycin	6.25	–	–	–	–	–	–	–	–
Ciprofloxacin	3.125	10.0	10.0	10.0	10.0	10.0	10.0	10.0	10.0
Fluconazole	–	–	–	–	–	30.0	30.0	30.0	30.0

'–'Indicates bacteria were resistant to the compound >100 μg/mL

[a] *S. aureus*

[b] *B. subtilis*

[c] *E. coli*

[d] *P. aeruginosa*

[e] *A. fumigatus*

[f] *A. niger*

[g] *A. flavus*

[h] *C. Albicans*

compounds **2k**, **2l**, **2m,** and **2n** were found to be more active compared to the activity of the compounds with fluoro atom on phenyl ring D (**2a**, **2c**, **2d,** and **2e)**. Certainly, the potency of the molecules was decreased on substitution of fluoro atom on phenyl ring 'D'. The compounds **2f** ($R_2 = H$, $R_3 = F$) and **2j** (R_2, $R_3 = F$) have shown the similar MIC (μg/mL) values. It indicates that, the activity of the molecules was not based on the number of fluoro atoms on phenyl ring 'D' and it was only due to the substitution on phenyl ring 'A'. Among the compounds with fluoro atom on phenyl ring D, the compound **2g** has shown the comparable activity as that of the streptomycin. It was concluded from the above facts that, the activity of molecules mainly depended on substitution on phenyl ring 'A' and phenyl ring 'C'. The reactivity of electron withdrawing and electron donating groups has been found in the order, $Cl > H > F > Br$ and $CH_3 < H < Cl$.

Antimicrobial studies

Most of the synthesized compounds were active against the Gram-positive bacteria *Bacillus subtilis* and Gram-negative bacteria *Pseudomonas aeruginosa* (Table 1). The compounds with fluoro atom on phenyl ring D (**2a**, **2b**, **2c**, **2h,** and **2i)**, have shown the higher potency compared to the compounds with neat phenyl ring D (**2m** and **2n)**. The compound **2a** ($R_3 = F$) has exhibited a good potency compared to compound **2n** ($R_3 = H$). None of the molecules have shown the MIC value equal to that of ciprofloxacin.

Some of the for pyrazoline derivatives integrated with sulfonamide scaffold were active against the *Aspergillus niger* and *Aspergillus flavus* (Table 1). The compounds **2c**, **2e,** and **2i** have shown the good activity over all fungi. When the activity was compared with the standard drug, the compound **2i** (R_2, $R_3 = F$) has shown the threefold more

Table 2 Crystal and structure refinement data for compounds **2e** and **2g**

Parameter	Value Compound **2e**	Value Compound **2g**
CCDC deposit no.	1,054,672	1,056,212
Empirical formula	$C_{23}H_{21}FN_4O_4S$	$C_{23}H_{20}F_2N_4O_4S$
Formula weight	468.50	486.49
Temperature	293(2) K	293(2) K
Wavelength	1.54178 Å	1.54178 Å
Crystal system, space group	Monoclinic, C2/*c*	Monoclinic, $P2_1/n$
Unit cell dimensions	$a = 10.293(2)$ Å	$a = 7.6673(14)$ Å
	$b = 23.397(5)$ Å	$b = 22.900(4)$ Å
	$c = 19.150(4)$ Å	$c = 12.874(2)$ Å
	$\beta = 102.424(11)°$	$\beta = 95.122(6)°$
Volume	4503.7(16) $Å^3$	2251.3(7) $Å^3$
Z, Calculated density	8, 1.382 Mg/m^3	4, 1.435 Mg/m^3
Absorption correction	Multi-scan	Multi-scan
Absorption coefficient	1.680 mm^{-1}	1.769 mm^{-1}
$F_{(000)}$	1952	1008
Crystal size	0.25 × 0.25 × 0.25 mm	0.25 × 0.25 × 0.25 mm
ϕ range for data collection	3.78° to 64.21°	6.11° to 64.48°
Limiting indices	$-10 \le h \le 11$	$-8 \le h \le 8$
	$-23 \le k \le 26$	$-26 \le k \le 26$
	$-20 \le l \le 21$	$-14 \le l \le 15$
Reflections collected/unique	11,312/3654 [R(int) = 0.0430]	21,534/3693 [R(int) = 0.0384]
Refinement method	Full-matrix least-squares on F^2	Full-matrix least-squares on F^2
Data/restraints/parameters	3654/0/300	3693/0/308
Goodness-of-fit on F^2	1.034	1.043
Final R indices [I > 2σ(I)]	$R1 = 0.0497$, w$R2 = 0.1405$	$R1 = 0.0431$, w$R2 = 0.1213$
R indices (all data)	$R1 = 0.0575$, w$R2 = 0.1481$	$R1 = 0.0451$, w$R2 = 0.1236$
Largest diff. peak and hole	0.390 and −0.431 e $Å^{-3}$	0.321 and −0.461 e $Å^{-3}$

potency against the *Aspergillus flavus* and 1.2-fold more potency against the *Candida albicans*, also the compounds **2c** and **2e** have shown 1.2-fold more potency against *Aspergillus niger*. It was concluded that, the potency of molecules increases with the increase in fluoro atoms on phenyl ring 'D'. On substitution of bromo (**2c**) and chloro (**2d**) atom at R position, a noticeable increase in the potency was observed.

*Crystal structure analysis of compounds **2e** and **2g***

The details of the crystal structure and data refinement were given in Table 2. The list of bond lengths and bond angles of the non-hydrogen atoms were given in Tables 3 and 4, respectively. Figs 2 and 3 represent the ORTEP diagram of the molecules **2e** and **2g** with thermal ellipsoids drawn at 50% probability, respectively.

In the compound **2e**, the central pyrazoline ring adopts a twisted conformation on the C3–C4 bond and its mean plane makes dihedral angles of 7.80(13)°, 71.14(15)°, and 75.48(12)° with the phenyl, 4-fluorophenyl, and 4-methoxyphenyl rings, respectively. In the compound **2g**, a study of torsion angles, asymmetric parameters and least-squares calculations reveals that, the pyrazoline ring adopts

Table 3 Bond length (Å) of some selected bonds of compounds **2e** and **2g**

Atoms	**2e**	**2g**
N1–C2	1.283(3)	1.357(2)
N1–N5	1.396(3)	1.389(2)
C2–C3	1.508(3)	1.539(2)
C4–N5	1.471(3)	1.287(2)
N5–C12	1.349(3)	1.484(2)
C12–O13	1.226(3)	1.218(2)
C12–N14	1.373(3)	1.373(2)
N14–N15	1.406(3)	1.402(2)
N15–S16	1.657(19)	1.643(18)
S16–C19	1.756(3)	1.761(2)

Table 4 Bond angle (°) of some selected bonds of compounds **2e** and **2g**

Atoms	**2e**	Atoms	**2g**
C2–N1–N5	107.72(16)	C2-N1-N5	107.2(2)
N1–C2–C6	123.46(19)	N1-C2-C6	122.3(2)
N1–C2–C3	112.7(2)	N1-C2-C3	114.0(2)
C6–C2–C3	123.84(19)	C6-C2-C3	123.6(2)
C2–C3–C4	103.24(16)	C2-C3-C4	104.2(2)
N5–C4–C26	113.48(17)	N5-C4-C27	113.16(19)
N5–C4–C3	99.48(16)	N5-C4-C3	100.33(18)
C26–C4–C3	111.96(19)	C27-C4-C3	115.5(2)
C12–N5–N1	122.80(17)	C12-N5-N1	122.1(2)
C12–N5–C4	123.78(18)	C12-N5-C4	121.16(19)
N1–N5–C4	113.37(16)	N1-N5-C4	113.96(18)
C11–C6–C2	120.1(2)	C11-C6-C2	120.3(3)
O13–C12–N5	122.46(19)	O13-C12-N5	120.7(2)
O13–C12–N14	122.0(2)	O13-C12-N14	122.7(2)
N5–C12–N14	115.51(19)	N5-C12-N14	116.6(2)
C12–N14–N15	114.17(18)	C12-N14-N15	117.00(18)
N14–N15–S16	112.19(14)	N14-N15-S16	114.58(15)
O18–S16–O17	120.15(11)	O18-S16-O17	120.23(11)
O18–S16–N15	104.02(10)	O18-S16-N15	104.73(11)
O17–S16–N15	106.72(11)	O17-S16-N15	104.66(10)
O18–S16–C19	108.99(12)	O18-S16-C19	110.22(12)
O17–S16–C19	107.85(11)	O17-S16-C19	106.82(12)
N15–S16–C19	108.61(10)	N15-S16-C19	107.98(8)
F25–C22–C21	119.0(3)	F25-C22-C21	119.1(3)
F25–C22–C23	118.1(3)	F25-C22-C23	117.2(3)

an envelope conformation on C4 and its mean plane makes dihedral angles of 15.34(10)°, 65.65(10)°, and 88.73(11)° with the phenyl, 2,4-difluorophenyl and 2-methoxyphenyl rings, respectively. The geometry around the S atom was distorted from regular tetrahedron, with the largest deviation observed for the O-S-O [O17-S16-O18 = 120.15(11)° and 120.23(11)° for compounds **2e** and **2g**, respectively] and O-S-N angle [O17-S16-N15 = 106.72(11)° and 104.66(10)° for compounds **2e** and **2g**, respectively]. This widening of the angles was due to the repulsive interactions between the S=O bonds and the non-bonded interactions involving the two S–O bonds and the varied steric hindrance of the substituent's. The value of bond angles N15-S16-C19 was 108.61(10)° and 107.98(8)°for the compounds **2e** and **2g,** respectively, which was comparable with the ideal tetrahedral value of 109.47°and was attributed to the Thorpe-Ingold effect (Bassindale 1984). Both the structures possess a chiral center at C4 with *R* conformation. Since the molecules have crystallized in a centrosymmetric space group, we can summarize that the compounds crystallize as a recemate.

In the compounds **2e** and **2g**, the structures exhibit both inter and intramolecular hydrogen bonds of the type N--H···N, C--H…O, C--H…N and N--H…N, N--H…O, C--H…F, C—H…O respectively, which play a vital role in stabilizing the crystal structure. In both the structures, the intra molecular hydrogen bonds N15--H15…O13 and N14--H14…N1 were closed to form a *S(6)* ring motif, whereas the N14--H14…O17 hydrogen bond links pairs of molecules related by inversion, forming the familiar $R^2_2(10)$ ring motif. In the compound **2e**, the packing of the molecule, when viewed along the *c* axis indicates that the molecules were interlinked by the intermolecular hydrogen bonds to form a chain like structure (Fig. 4), whereas, for the compound **2g**, the packing of the molecule indicates that they were interconnected by these hydrogen bonds to form a zig-zag structure (Figs 5 and 6).

Hirshfeld surface analysis

The Hirshfeld surface analysis comprising of the d_{norm} surface plots, electrostatic potentials and the two-dimensional fingerprint plots (FPs) were generated in order to quantify and give visual confirmation of the intermolecular interactions and to explain the observed crystal structures (Tables 5 and 6). The quantitative analysis of the intermolecular interactions can be made by comparing the FPs of the compounds **2e** and **2g** (Fig. 7). The full FP of each compound was different in both size and shape, thus indicating that, the nature and separation of the various interatomic contacts in the two compounds were very different. The FP for different atom…atom contacts in compounds **2e** and **2g** and the percentage contribution of each contacts to the Hirshfeld surfaces of compounds (Fig. 8) showed that, the greatest contribution was due to H…H contacts (i.e., dispersive forces), followed by H…C, H…O, and H…F contacts in each structure. The FP plot for the compound **2e** features a pair of long sharp spikes characteristic of a strong hydrogen bond at $d_i + d_e \approx 2.2$ Å, whereas in compound **2g** similar sharp spikes occur at a relatively shorter contact distance $d_i + d_e \approx 2.0$ Å, indicating that the hydrogen bonds in compound **2g** were shorter and stronger than those in compound **2e**. The crystal structure of compound **2e** features H…H contacts, with $de_{mini} = di_{mini} \cong 1.1$ Å, while in compound **2g**, these contacts appear at $de_{mini} = di_{mini} \cong 1$ Å. Also, noteworthy was that the FP for the H…H contact of compound **2g** was slightly broader than that of compound **2e**. This illustrates that, the H…H contacts in compound **2e** were the result of a head-on approach, while in compound **2g**, it is more or less due to the side-ways approach. Further, the presence of C–H…π and π…π interactions in both the structures was established by investigating the FP for both compounds.

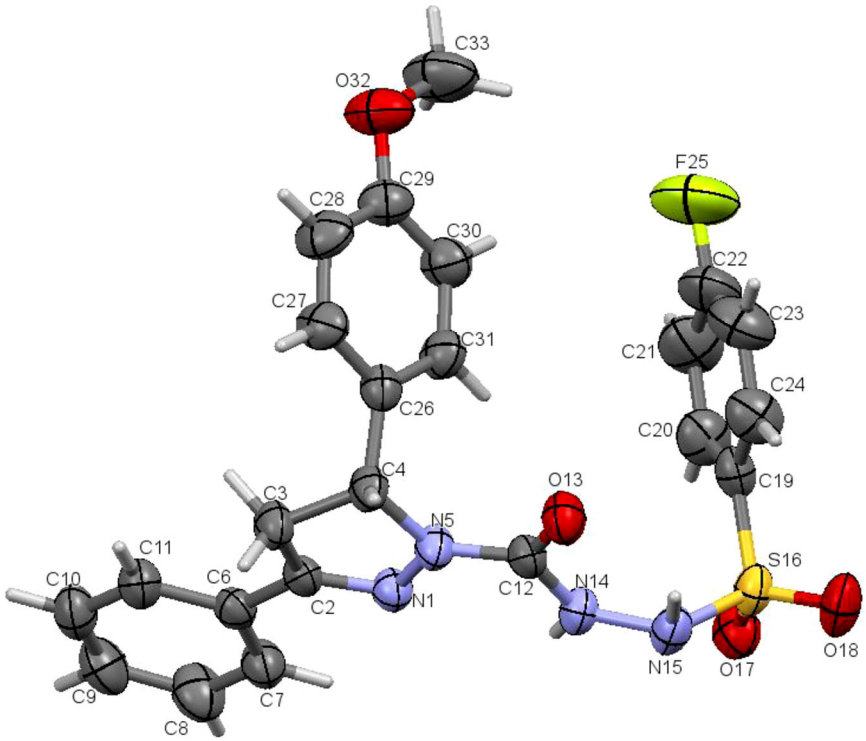

Fig. 2 ORTEP diagram of the compound **2e** with thermal ellipsoids drawn at 50% probability

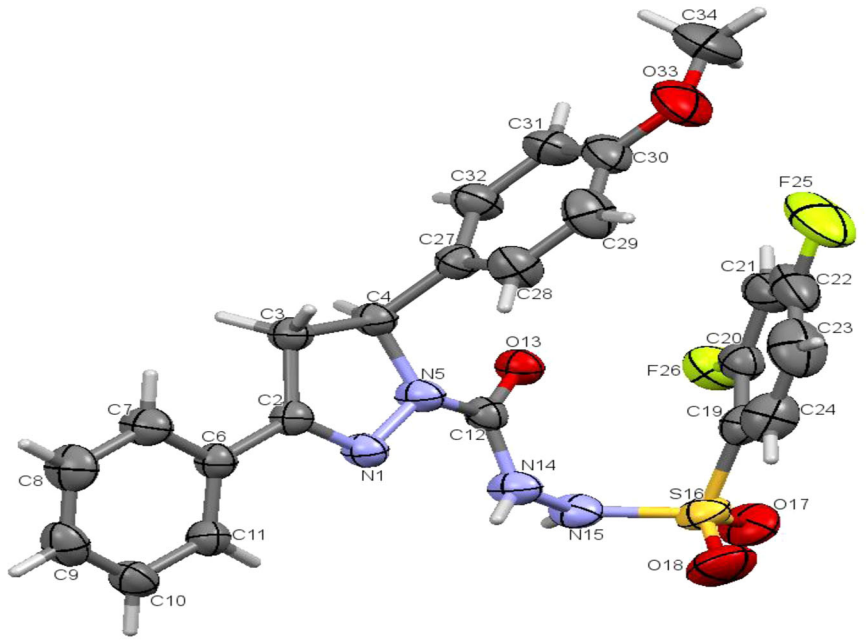

Fig. 3 ORTEP diagram of the compound **2g** with thermal ellipsoids drawn at 50% probability

Conclusions

In the present study, fourteen pyrazoline derivatives integrated with sulfonamide scaffold were synthesized and structurally characterized by elemental analysis, UV–Vis, IR, NMR, and mass spectra. The results of single crystal X-ray diffraction study of the compounds **2e** and **2g** was revealed that, the molecules exhibit both inter and intramolecular hydrogen bonds of the type N--H···N, C--H…O, C--H…N, and N--H…N, N--H…O, C--H…F, C--H…O respectively, which play a vital role in stabilizing the crystal structure. The FP for different atom…atom contacts in

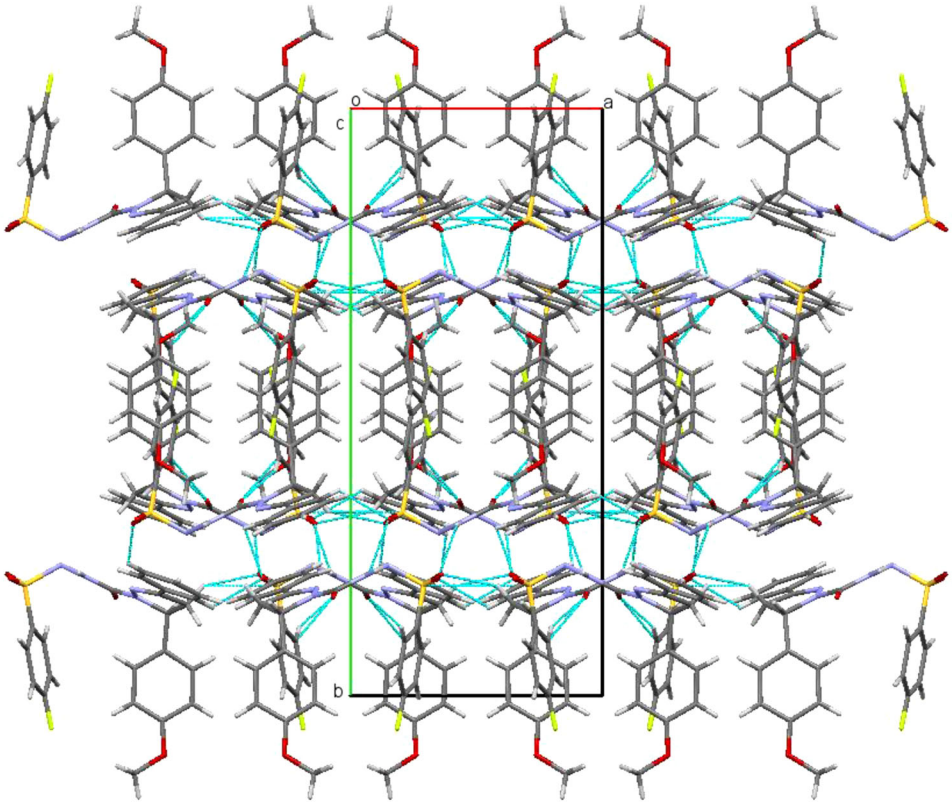

Fig. 4 Packing of the compound **2e**, when viewed down along the *c* axis. The *dotted lines* indicate hydrogen bonds

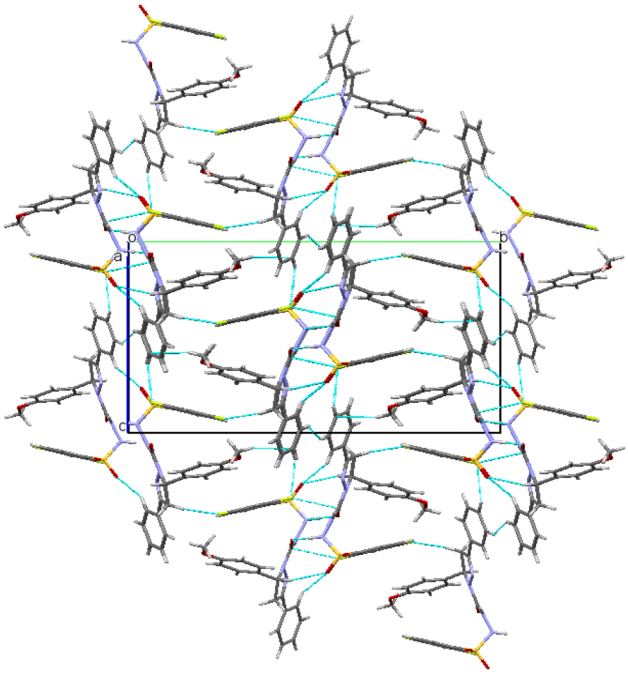

Fig. 5 Packing of the compound **2g**, when viewed down along the *c* axis. The *dotted lines* indicate hydrogen bonds

compounds **2e** and **2g** and the percentage contribution of each contacts to the Hirshfeld surfaces of compounds showed that the greatest contribution was due to H…H contacts followed by H…C, H…O and H…F contacts. The compounds **2m** and **2n** have shown the best effect over the growth of *M. tuberculosis*. The SAR of the compounds revealed that the antitubercular activity of the synthesized compounds decreased with the introduction of fluoro atoms on phenyl ring 'D'. Majority of the compounds have shown remarkable high potential antimicrobial activity. The antimicrobial activity of the pyrazoline derivatives integrated with sulfonamide scaffold was enhanced with the introduction of fluoro atom on phenyl ring 'D'. This research work has an influence on further exploration of the title compound in the field of drug discovery.

Materials and methods

Chemistry

All the reactions were carried out in oven dried glassware and under nitrogen atmosphere. Melting point was determined by an open capillary method and was uncorrected. The chemicals used for the reaction were from Sigma-Aldrich Chemical Pvt. Ltd. Bengaluru, India. The reactions were monitored by thin-layer chromatography (TLC) using recoated silica gel $60F_{254}$ plates (Merck) and 40% ethyl acetate in petroleum ether was used as mobile phase. Purity of the synthesized compounds was confirmed by TLC.

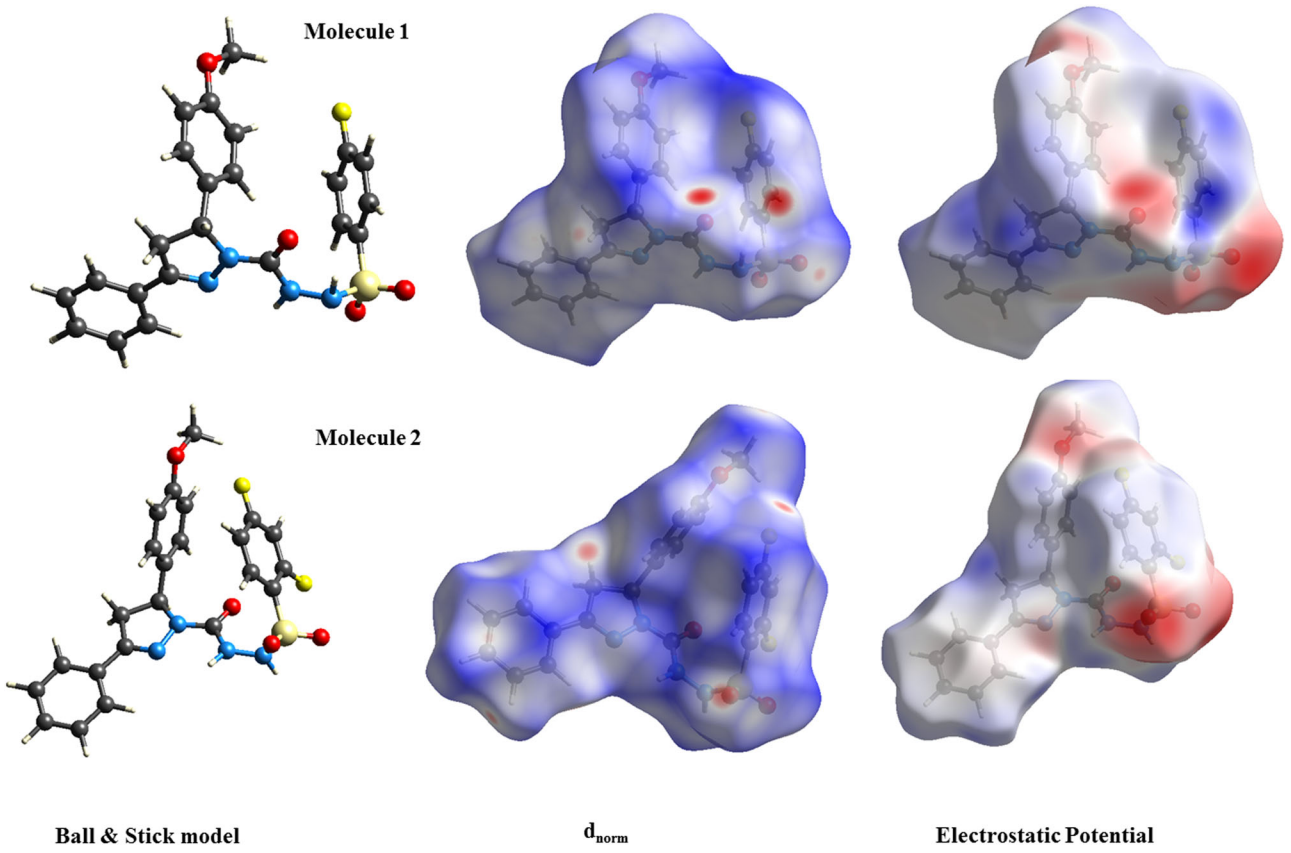

Fig. 6 d_{norm} and electrostatic potential mapped on Hirshfeld surface for visualizing the intermolecular contacts in compounds **2e** (molecule 1) and **2g** (molecule 2)

Table 5 Hydrogen bond geometry for compound **2e** (Å, °)

D—H···A	*d* (D—H)	*d* (H···A)	*d* (D···A)	<(DHA)
N14--H14···N1	0.86	2.39	2.698 (3)	101
N14--H14···O17$^{(i)}$	0.86	2.53	3.113 (3)	126
N15--H15···O13	1.01	2.00	2.617 (3)	117
C3—H3A…O18$^{(ii)}$	0.97	2.59	3.397 (3)	140
C8—H8…O18 $^{(iii)}$	0.93	2.59	3.262 (4)	130
C20—H20…O17	0.93	2.53	2.900 (3)	104
C24—H24…O13$^{(iv)}$	0.93	2.35	3.212 (3)	154
C31—H31···N5	0.82	2.53	2.877 (3)	103

Symmetry codes: (i) $3/2 - x, 3/2 - y, 1 - z$; (ii) $-1 + x, y, z$; (iii) $-1/2 + x, 3/2 - y, 1/2 + z$; (iv) $1 - x, y, 1/2 - z$

Table 6 Hydrogen bond geometry for compound **2g** (Å, °)

D—H···A	*d* (D—H)	*d* (H···A)	*d* (D···A)	<(DHA)
N14--H14···N1	0.86	2.37	2.685 (2)	102
N15--H15···O13$^{(i)}$	0.86	2.26	2.870 (2)	128
C3—H3A…F25$^{(ii)}$	0.97	2.45	3.345 (3)	153
C11—H11…O17$^{(iii)}$	0.93	2.43	3.242 (2)	145
C21—H21…O18$^{(iv)}$	0.93	2.50	3.358 (3)	154
C24—H24…O18	0.93	2.49	2.869 (3)	105

Symmetry codes: (i) $1 - x, -y, 2 - z$; (ii) $1/2 + x, 1/2 - y, 1/2 + z$; (iii) $2 - x, -y, 2 - z$; (iv) $-1 + x, y, z$

Spots were detected by their absorption under UV light. The elemental analysis and spectra were recorded in analytical lab, Sigma-Aldrich Chemical Pvt. Ltd. Bengaluru, India. Elemental analysis was performed on Leco-932 CHNS analyzer. The UV–Vis spectra of the compounds were determined using Perkin-Elemer lambda spectrometer and methanol was used as solvent. IR spectra were recorded in Perkin Elmer Fourier transform infrared spectroscopy (FTIR) 100 series spectrometer. Samples were dried at 100 °C, under vacuum for 24 h and 16 scans were averaged across the spectral range of 400–4000 cm^{-1}. The IR stretching frequency of the important functional groups was reported in cm^{-1}. The NMR spectra of the compounds were recorded on a Bruker amx 400 spectrometer operating at 400 and 100 MHz for ^{1}H and ^{13}C nuclei, respectively. The chemical shifts were given in ppm, coupling constant (*J*) values were presented in hertz (Hz) and the abbreviations were as follows: s (singlet), d (doublet), t (triplet), and

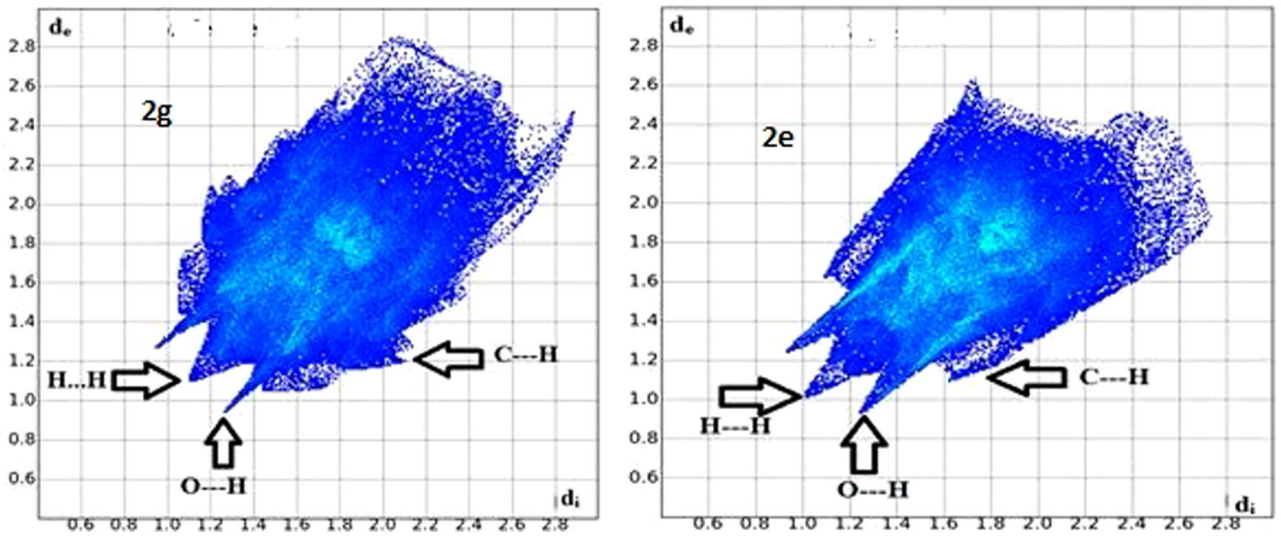

Fig. 7 Comparison of the FP for each of compounds **2e** and **2g**. d_i was the closest internal distance from a given point on the Hirshfeld surface and d_e was the closest external contacts

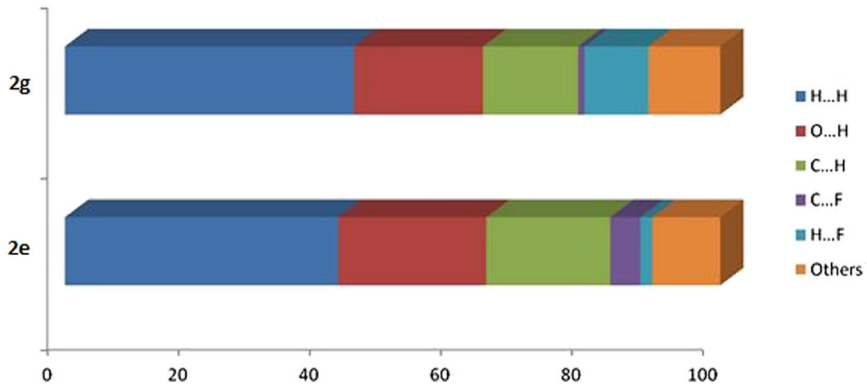

Fig. 8 Percentage contributions of the various intermolecular contacts contributing to the Hirshfeld surfaces of compounds **2e** and **2g**

m (multiplets). The mass spectra of compounds were recorded on Agilent LC/MVD XCT plus mass spectrometer.

Synthesis of the pyrazoline derivatives integrated with sulfonamide scaffold (2a–n)

The *N*-methyl ester pyrazolines were synthesized from the corresponding chalcones **1a–n** by utilizing the process mentioned in the literature (Raghav and Singh 2014). These pyrazoline derivatives was converted into corresponding carbohydrazide derivatives by the reaction with hydrazine hydrate at reflux temperature in methanol as mentioned in the literature (Wu et al. 2013).

The mixture of appropriate pyrazoline derivative (1.00 mmol) and pyridine (2.00 mmol) was dissolved in dichloromethane. The reaction mass was cooled to 5 °C and fluoro substituted benene sulfonyl chloride (1.02 mmol) was added. The reaction mass was allowed to stir for 2 h at 5 °C. The progress of the reaction was monitored using TLC. The product was extracted with ethyl acetate. The solvent removed under vacuum and the final product was recrystallized using ethanol. The physical properties, overall yields, spectral data of synthesized compounds were listed below.

N'-*(4-fluorobenzenesulfonyl)-3,5-diphenyl-4,5-dihydro-1H-pyrazole-1-carbohydrazide (**2a**)*

Light-yellow crystals. Yield: 65%; m.p. 186–187 °C; UV–Vis λ_{max} (nm): 296.30, 217.58; FTIR stretching frequencies (cm^{-1}): 1154.72 and 1342.12 (S=O), 1430.91 (C=N), 1673.18 (C=O), 3343.95 (N–H), 3677.16 (N–H); ^{1}H NMR (400 MHz, DMSO-d_6) δ (ppm): 3.02–3.07 (dd, 1H, pyrazoline CH_aH, $J = 5.0$ Hz, 18.2 Hz), 3.74–3.82 (dd, 1H, pyrazoline CHH_b, $J = 12.0$ Hz, 18.0 Hz), 5.25–5.29 (dd,

1H, pyrazoline CH_c, $J = 5.2$ Hz, 12.0 Hz), 7.02–7.05 (m, 2H, CH arom), 7.21–7.31 (m, 5H, CH arom), 7.43–7.44 (m, 3H, CH arom), 7.79–7.84 (m, 4H, CH arom), 9.39 (s, 1H, NH_{2N}), 9.68 (s, 1H, NH_{1N}); ^{13}C NMR (100 MHz, DMSO-d_6) δ (ppm): 41.39, 60.28, 115.76, 125.28, 126.77, 127.01, 128.42, 128.53, 129.97, 130.55, 130.64, 131.12, 135.64, 142.41, 152.50, 163.12; Anal. Calcd for $C_{22}H_{19}FN_4O_3S$: C, 60.26; H, 4.37; N, 12.78; S, 7.37. Found: C, 60.27; H, 4.38; N, 12.76; S, 6.09; ESI MS: $m/z = 439.2$ $[M + H]^+$.

N'-*(4-fluorobenzenesulfonyl)-5-(4-fluorophenyl)-3-phenyl-4,5-dihydro-1H-pyrazole-1-carbohydrazide (**2b**)*

Light-yellow crystalline solid. Yield: 82%; m.p. 228–229 °C; UV–Vis λ_{max} (nm): 296.74, 219.80; FTIR stretching frequencies (cm^{-1}): 1154.80 and 1342.32 (S=O), 1486.73 (C=N), 1675.52 (C=O), 2882.09 (CH arom), 3108.96 (N–H), 3414.14 (N–H); ^{1}H NMR (400 MHz, DMSO-d_6) δ (ppm): 2.85–2.90 (dd, 1H, pyrazoline CH_aH, $J = 5.6$ Hz, 18.0 Hz), 3.54–3.62 (dd, 1H, pyrazoline CHH_b, $J = 12.0$ Hz, 18.4 Hz), 5.07–5.11 (dd, 1H, pyrazoline CH, $J = 5.2$ Hz, 12.8 Hz), 6.87–6.95 (m, 4H, CH arom), 7.07–7.12 (m, 2H, CH arom), 7.25–7.27 (m, 3H, CH arom), 7.61–7.67 (m, 4H, CH arom), 9.19 (s, 1H, NH_{2N}), 9.47 (s, 1H, NH_{1N}); ^{13}C NMR (100 MHz, DMSO-d_6) δ (ppm): 41.61, 59.68, 115.13, 115.70, 126.80, 127.46, 128.54, 130.01, 130.64, 131.08, 135.52, 138.58, 152.33, 152.69, 159.99, 163.03; Anal. Calcd for $C_{22}H_{18}F_2N_4O_3S$: C, 57.89; H, 3.97; N, 12.27; S, 7.02. Found: C, 57.90; H, 3.94; N, 12.29; S, 7.12; ESI MS: $m/z = 457.2$ $[M + H]^+$.

5-(4-bromophenyl)-N'-*(2,4-difluorobenzenesulfonyl)-3-phenyl-4,5-dihydro-1H-pyrazole-1-carbohydrazide (**2c**)*

Light-brown powder. Yield: 72%; m.p. 224–225 °C; UV–Vis λ_{max} (nm): 298.52, 219.80; FTIR stretching frequencies (cm^{-1}): 1162.85 and 1348.97 (S=O), 1471.76 (C=N), 1675.41 (C=O), 2883.29 (CH arom), 3101.19 (N–H), 3404.71 (N–H); ^{1}H NMR (400 MHz, DMSO-d_6) δ (ppm): 3.01–3.07 (dd, 1H, pyrazoline CH_aH, $J = 5.4$ Hz, 18.2 Hz), 3.73–3.80 (dd, 1H, pyrazoline CHH_b, $J = 12.0$ Hz, 18.0 Hz), 5.22–5.27 (dd, 1H, pyrazoline CH_c, $J = 5.6$ Hz, 12.0 Hz), 6.94–6.97 (m, 2H, CH arom), 7.08–7.13 (m, 1H, CH arom), 7.27–7.33 (m, 1H, CH arom), 7.42–7.49 (m, 5H, CH arom), 7.75–7.84 (m, 3H, CH arom), 9.48 (s, 1H, NH_{2N}), 9.93(s, 1H, NH_{1N}); ^{13}C NMR (100 MHz, DMSO-d_6) δ (ppm):41.38, 59.79, 105.38, 111.32, 120.07, 124.02, 126.80, 127.60, 128.54, 130.04, 130.99, 131.30, 132.37, 141.71, 152.38, 152.67, 158.80, 163.95; Anal. Calcd. for $C_{22}H_{17}BrF_2N_4O_3S$: C, 49.36; H, 3.20; N, 10.47; S, 5.99. Found: C, 49.34; H, 3.21; N, 10.45; S, 6.10; ESI MS: $m/z =$ 534.9 $[M + H]^+$.

5-(4-chlorophenyl)-N'-*(4-fluorobenzenesulfonyl)-3-phenyl-4,5-dihydro-1H-pyrazole-1-carbohydrazide (**2d**)*

White crystalline solid. Yield: 72%; m.p. 231–232 °C; UV–Vis λ_{max} (nm): 294.96, 220.24; FTIR stretching frequencies (cm^{-1}): 1167.78 and 1342.30 (S=O), 1468.89 (C=N), 1677.03 (C=O), 2879.78 (CH arom), 3117.98 (N–H), 3414.10 (N–H); ^{1}H NMR (400 MHz, DMSO-d_6) δ (ppm): 3.09–3.15 (dd, 1H, pyrazoline CH_aH, $J = 5.6$ Hz, 18.0 Hz), 3.80–3.87 (dd, 1H, pyrazoline CHH_b, $J = 12.2$ Hz, 17.8 Hz), 5.31–5.35 (dd, 1H, pyrazoline CH_c, $J = 5.4$ Hz, 11.8 Hz), 7.10–7.13 (dd, 2H, CH arom, $J = 2.2$ Hz, 8.6 Hz), 7.31–7.36 (m, 2H, CH arom), 7.40–7.42 (dd, 2H, CH arom, $J = 2.2$ Hz, 8.2 Hz), 7.50–7.51 (t, 3H, CH arom, $J =$ 3.2 Hz), 7.85–7.91 (m, 4H, CH arom), 9.45 (s, 1H, NH_{2N}), 9.71 (s, 1H, NH_{1N}); ^{13}C NMR (100 MHz, DMSO-d_6) δ (ppm): 41.47, 59.70, 115.71, 126.79, 127.36, 128.38, 128.54, 130.04, 130.63, 131.03, 131.62, 135.51, 141.32, 152.35, 152.66, 163.08; Anal. Calcd for $C_{22}H_{18}ClFN_4O_3S$: C, 55.87; H, 3.84; N, 11.85; S, 6.78. Found: C, 55.85; H, 3.86; N, 11.82; S, 6.45; ESI MS: $m/z = 471.0$ $[M + H]^+$.

N'-*(4-fluorobenzenesulfonyl)-5-(4-methoxyphenyl)-3-phenyl-4,5-dihydro-1H-pyrazole-1-carbohydrazide (**2e**)*

Light-pink color powder. Yield: 62%; m.p. 196–197 °C; UV–Vis λ_{max} (nm): 298.08, 223.36; FTIR stretching frequencies (cm^{-1}): 1169.56 and 1423.93 (S = O), 1482.60 (C = N), 1667.86 (C = O), 2967.77 (CH_3), 3063.02 (CH arom), 3100.90 (CH arom), 3176.75 (N–H), 3354.01 (N–H);^{1}H NMR (400 MHz, DMSO-d_6) δ (ppm): 3.07–3.12 (dd, 1H, pyrazoline CH_aH, $J = 5.2$ Hz, 17.6 Hz), 3.76–3.84 (dd, 1H, pyrazoline CHH_b, $J = 11.8$ Hz, 17.8 Hz), 3.79 (s, 3H, CH_3), 5.26–5.30 (dd, 1H, pyrazoline CH_c, $J = 5.2$ Hz, 12.2 Hz), 6.89–6.91 (d, 2H, CH arom, $J = 8.4$ Hz), 7.01–7.03 (d, 2H, CH arom, $J = 8.8$ Hz), 7.32–7.36 (m, 2H, CH arom), 7.49–7.51 (t, 3H, CH arom, $J = 3.2$ Hz), 7.85–7.91 (m, 4H, CH arom), 9.37 (s, 1H, NH_{2N}), 9.69 (s, 1H, NH_{1N}); ^{13}C NMR (100 MHz, DMSO-d_6) δ (ppm): 41.66, 55.07, 59.83, 113.78, 115.71, 126.61, 126.76, 128.54, 129.94, 130.60, 131.20, 134.45, 135.58, 152.26, 152.63, 158.34, 163.07; Anal. Calcd for $C_{23}H_{21}FN_4O_4S$: C, 58.96; H, 4.52; N, 11.96; S, 6.84. Found: C, 58.92; H, 4.50; N, 11.94; S, 6.73; ESI MS: $m/z = 469.2$ $[M + H]^+$.

N'-*(4-fluorobenzenesulfonyl)-5-(4-methylphenyl)-3-phenyl-4,5-dihydro-1H-pyrazole-1-carbohydrazide (**2f**)*

White powder. Yield: 75%; m.p. 212–213 °C; UV–Vis λ_{max} (nm): 297.19, 219.35; FTIR stretching frequencies (cm^{-1}): 1169.16 and 1342.68 (S=O), 1492.56 (C=N), 1672.52 (C=O), 3059.06 (CH_3), 3241.77 (N–H), 3416.03 (N–H); ^{1}H NMR (400 MHz, DMSO-d_6) δ (ppm): 2.33 (s, 3H, CH_3) 3.05–3.11

(dd, 1H, pyrazoline CH_aH, $J = 5.4$ Hz, 17.8 Hz), 3.78–3.85 (dd, 1H, pyrazoline CHH_b, $J = 11.8$ Hz, 17.8 Hz), 5.27–5.31 (dd, 1H, pyrazoline CH_c, $J = 5.2$ Hz, 12.0 Hz), 6.97–6.99 (d, 2H, CH arom, $J = 8.4$ Hz), 7.14–7.16 (d, 2H, CH arom, $J = 8.8$ Hz), 7.35–7.35 (t, 2H, CH arom, $J = 9.2$ Hz), 7.49–7.51 (m, 3H, CH arom), 7.85–7.90 (m, 4H, CH arom), 9.38 (s, 1H, NH_{2N}), 9.67 (s, 1H, NH_{1N}); ^{13}C NMR (100 MHz, DMSO-d_6) δ (ppm): 20.58, 41.66, 60.09, 115.72, 125.26, 126.74, 128.55, 128.93, 129.94, 130.58, 131.16, 135.58, 136.18, 139.53, 152.27, 152.64, 163.20; Anal. Calcd for $C_{23}H_{21}FN_4O_3S$: C, 61.05; H, 4.68; N, 12.38; S, 7.09. Found: C, 61.07; H, 4.70; N, 12.35; S, 7.10; ESI MS: $m/z = 453.2$ $[M + H]^+$.

N'-*(2,4-difluorobenzenesulfonyl)-5-(4-methoxyphenyl)-3-phenyl-4,5-dihydro-1H-pyrazole-1-carbohydrazide (**2g**)*

Light-brown crystalline solid. Yield: 68%; m.p. 197–198 °C; UV–Vis λ_{max} (nm): 295.41, 222.91; FTIR stretching frequencies (cm^{-1}): 1163.23 and 1351.6 (S=O), 1473.77 (C=N), 1672.81 (C=O), 2882.25 (CH_3), 3102.02 (N–H), 3405.91 (N–H); ^{1}H NMR (400 MHz, DMSO-d_6) δ (ppm): 3.00–3.05 (dd, 1H, pyrazoline CH_aH, $J = 5.2$ Hz, 18.0 Hz), 3.70–3.77 (dd, 1H, pyrazoline CHH_b, $J = 12.4$ Hz, 17.6 Hz), 3.73 (s, 3H, CH_3), 5.19–5.24 (dd, 1H, pyrazoline CH_c, $J = 5.2$ Hz, 12.0 Hz), 6.82–6.94 (dd, 4H, CH arom, $J = 8.8$ Hz, 39.2 Hz), 7.09–7.14 (m, 1H, CH arom), 7.30–7.36 (m, 1H, CH arom), 7.43–7.44 (m, 3H, CH arom), 7.76–7.84 (m, 3H, CH arom), 9.41 (s, 1H, NH_{2N}), 9.91 (s, 1H, NH_{1N}); ^{13}C NMR (100 MHz, DMSO-d_6) δ (ppm): 41.61, 55.02, 59.72, 105.51, 111.42, 113.73, 124.14, 126.52, 126.74, 128.53, 129.94, 131.17, 132.35, 134.34, 152.29, 152.64, 158.30, 161.34, 166.50; Anal. Calcd for $C_{23}H_{20}F_2N_4O_4S$: C, 56.78; H, 4.14; N, 11.52; S, 6.59. Found: C, 56.76; H, 4.16; N, 11.54; S, 6.65; ESI MS: $m/z = 487.2$ $[M + H]^+$.

N'-*(4-fluorobenzenesulfonyl)-3,5-bis(4-fluorophenyl)-4,5-dihydro-1H-pyrazole-1-carbohydrazide (**2h**)*

Brown solid. Yield: 80%; m.p. 227–228 °C; UV–Vis λ_{max} (nm): 293.19, 221.13; FTIR stretching frequencies (cm^{-1}): 1156.34 and 1339.85 (S=O), 1494.86 (C=N), 1689.74 (C=O), 3247.15 (N–H), 3440.55 (N–H); ^{1}H NMR (400 MHz, DMSO-d_6) δ (ppm): 2.94–3.00 (dd, 1H, pyrazoline CH_aH, $J = 5.6$ Hz, 18.0 Hz), 3.63–3.70 (dd, 1H, pyrazoline CHH_b, $J = 12.0$ Hz, 18.0 Hz), 5.16–5.20 (dd, 1H, pyrazoline CH_c, $J = 5.2$ Hz, 12.0 Hz), 6.96–7.05 (m, 4H, CH arom), 7.16–7.23 (m, 4H, CH arom), 7.70–7.73 (m, 2H, CH arom), 7.79–7.83 (m, 2H, CH arom),9.32 (s, 1H, NH_{2N}), 9.56 (s, 1H, NH_{1N}); ^{13}C NMR (100 MHz, DMSO-d_6) δ (ppm): 41.72, 59.80, 115.00, 115.22, 115.65, 127.46, 127.75, 129.13, 130.61, 135.49, 138.50, 151.44, 152.73, 160.02, 161.86, 163.12; Anal. Calcd for $C_{22}H_{16}F_4N_4O_3S$: C, 53.66; H, 3.28; N, 11.38; S, 6.76. Found: C, 53.67; H, 3.29; N, 11.34; S, 6.78; ESI MS: $m/z = 475.2$ $[M + H]^+$.

N'-*(2,4-difluorobenzenesulfonyl)-3,5-diphenyl-4,5-dihydro-1H-pyrazole-1-carbohydrazide (**2i**)*

Light-yellow powder. Yield: 70%; m.p. 189–190 °C; UV–Vis λ_{max} (nm): 297.19, 218.46; FTIR stretching frequencies (cm^{-1}): 1170.23 and 1348.77 (S=O), 1509.35 (C=N), 1653.77 (C=O), 3114.57 (N–H), 3356.97 (N–H); ^{1}H NMR (400 MHz, DMSO-d_6) δ (ppm): 3.07–3.13 (dd, 1H, pyrazoline CH_aH, $J = 5.2$ Hz, 18.0 Hz), 3.80–3.88 (dd, 1H, pyrazoline CHH_b, $J = 11.8$ Hz, 18.2 Hz), 5.31–5.35 (dd, 1H, pyrazoline CH_c, $J = 6.0$ Hz, 12.2 Hz), 7.06–7.08 (m, 2H, CH arom), 7.15–7.20 (m, 1H, CH arom), 7.26–7.40 (m, 4H, CH arom), 7.48–7.51 (m, 3H, CH arom), 7.83–7.91 (m, 3H, CH arom), 9.52 (s, 1H, NH_{2N}) 10.0 (s, 1H, NH_{1N}); ^{13}C NMR (100 MHz, DMSO-d_6) δ (ppm): 40.29, 58.79, 104.11, 109.94, 122.66, 123.80, 125.36, 125.56, 126.97, 127.10, 128.55, 129.69, 130.84, 140.88, 150.91, 151.35, 157.35, 162.44; Anal. Calcd for $C_{22}H_{18}F_2N_4O_3S$: C, 57.89; H, 3.97; N, 12.27; S, 7.02. Found: C, 57.87; H, 3.96; N, 12.28; S, 7.05; ESI MS: $m/z = 457.2$ $[M + H]^+$.

N'-*(2,4-difluorobenzenesulfonyl)-5-(4-methylphenyl)-3-phenyl-4,5-dihydro-1H-pyrazole-1-carbohydrazide (**2J**)*

Light-yellow crystals. Yield: 55%; m.p. 184–185 °C; UV–Vis λ_{max} (nm): 296.74, 217.13. FTIR stretching frequencies (cm^{-1}): 1169.70 and 1347.30 (S=O), 1506.00 (C=N), 1668.32 (C=O), 2884.30 (CH_3), 3104.00 (CH arom), 3404.61 (N–H), 3343.90 (N–H); ^{1}H NMR (400 MHz, DMSO-d_6) δ (ppm): 2.32 (s, 3H, CH_3), 3.01–3.09 (dd, 1H, pyrazoline CH_aH, $J = 5.2$ Hz, 12.8 Hz), 3.76–3.84 (dd, 1H, pyrazoline CHH_b, $J = 12.0$ Hz, 18.0 Hz), 5.25–5.30 (dd, 1H, pyrazoline CH_c, $J = 5.2$ Hz, 12.0 Hz), 6.93–6.95 (d, 2H, CH arom), 7.12–7.19 (m, 3H, CH arom), 7.34–7.39 (m, 1H, CH arom), 7.48–7.49 (m, 3H, CH arom), 7.81–7.89 (m, 3H, CH arom), 9.48 (s, 1H, NH_{2N}), 9.97 (s, 1H, NH_{1N}); ^{13}C NMR (100 MHz, DMSO-d_6) δ (ppm): 20.57, 41.65, 60.00, 105.48, 111.27, 124.02, 125.20, 126.74, 128.53, 128.90, 129.92, 131.15, 132.26, 136.09, 139.36, 152.25, 152.68, 161.32; Anal. Calcd for $C_{23}H_{20}F_2N_4O_3S$: C, 58.72; H, 4.28; N, 11.91; S, 6.81. Found: C, 58.70; H, 4.25; N, 11.92; S, 6.89; ESI MS: $m/z = 471.2$ $[M + H]^+$.

N'-*(benzenesulfonyl)-5-(4-bromophenyl)-3-phenyl-4,5-dihydro-1H-pyrazole-1-carbohydrazide (**2k**)*

White powder. Yield: 68%; m.p. 227–228 °C; UV–Vis λ_{max} (nm): 296.30, 220.24; FTIR stretching frequencies (cm^{-1}): 1165.90 and 1338.25 (S=O), 1505.92 (C=N), 1676.48 (C=O), 3211.46 (N–H), 3345.36 (N–H). ^{1}H NMR (400

MHz, DMSO-d_6) δ (ppm): 3.09–3.15 (dd, 1H, pyrazoline CH_aH, $J = 5.6$ Hz, 18.0 Hz), 3.80–3.87 (dd, 1H, pyrazoline CHH_b, $J = 12.0$ Hz, 16.6 Hz), 5.30–5.34 (dd, 1H, pyrazoline CH_c, $J = 5.2$ Hz, 12.0 Hz), 7.06–7.08 (dd, 2H, CH arom, $J = 2.0$ Hz, 6.4 Hz), 7.49–7.51 (m, 3H, CH arom), 7.53–7.54 (m, 2H, CH arom), 7.55–7.56 (m, 2H, CH arom), 7.61–7.65 (m, 1H, CH arom), 7.82–7.84 (d, 2H, CH arom, $J = 7.6$ Hz), 7.87–7.90 (m, 2H, CH arom), 9.37 (s, 1H, NH_{2N}), 9.66 (s, 1H, NH_{1N}); ^{13}C NMR (100 MHz, DMSO-d_6) δ (ppm): 41.46, 59.79, 120.09, 126.79, 127.50, 127.78, 128.54, 128.60, 130.02, 131.04, 131.33, 132.51, 139.38, 141.86, 152.31, 152.75; Anal. Calcd for $C_{22}H_{19}BrN_4O_3S$: C, 52.91; H, 3.84; N, 11.22; S, 6.42. Found: C, 52.95; H, 3.88; N, 11.25; S, 6.49; ESI MS: $m/z =$ 499.38 $[M + H]^+$.

N'-*(benzenesulfonyl)-5-[4-(methylsulfanyl)phenyl]-3-phenyl-4,5-dihydro-1H-pyrazole-1-carbohydrazide* ***(2l)***

Light-yellow crystals. Yield: 60%; m.p. 175–176 °C; UV–Vis λ_{max} (nm): 294.07, 260.27, 217.58; FTIR stretching frequencies (cm^{-1}): 1166.51 and 1338.96 (S=O), 1505.83 (C=N), 1690.87 (C=O), 3059.10 (CH arom), 3248.35 (N–H), 3416.00 (N–H); ^{1}H NMR (400 MHz, DMSO-d_6) δ (ppm): 2.45 (s, 3H, CH_3), 3.01–3.07 (dd, 1H, pyrazoline CH_aH, $J = 5.2$ Hz, 18.0 Hz), 3.72–3.80 (dd, 1H, pyrazoline CHH_b, $J = 12.0$ Hz, 18.0 Hz), 5.22–5.26 (dd, 1H, pyrazoline CH_c, $J = 4.8$ Hz, 11.6 Hz), 6.98–7.00 (d, 2H, CH arom, $J = 8.4$ Hz), 7.17–7.19 (d, 2H, CH arom, $J =$ 8.4 Hz), 7.43–7.46 (m, 3H, CH arom), 7.48–7.50 (d, 2H, CH arom, $J = 7.6$ Hz), 7.56–7.59(m, 1H, CH arom), 7.76–7.78 (d, 2H, CH arom, $J = 7.6$ Hz), 7.81–7.83 (m, 2H, CH arom), 9.26 (s, 1H, NH_{2N}), 9.59 (s, 1H, NH_{1N}); ^{13}C NMR (100 MHz, DMSO-d_6) δ (ppm): 14.58, 41.54, 59.89, 126.09, 126.21, 126.76, 127.50, 128.55, 128.62, 129.96, 131.12, 132.54, 136.72, 139.72, 139.39, 152.24, 152.78; Anal. Calcd for $C_{23}H_{22}N_4O_3S_2$: C, 59.21; H, 4.75; N, 12.01. S, 13.74. Found: C, 59.25; H, 4.71; N, 12.04; S, 13.67; ESI MS: $m/z = 466.57$ $[M + H]^+$.

N'-*(benzenesulfonyl)-5-(4-chlorophenyl)-3-phenyl-4,5-dihydro-1H-pyrazole-1-carbohydrazide* ***(2m)***

Colorless crystals. Yield: 59%; m.p. 201–202 °C; UV–Vis λ_{max} (nm): 295.85, 220.24; FTIR stretching frequencies (cm^{-1}): 1163.76 and 1331.61 (S=O), 1504.44 (C=N), 1671.36 (C=O), 3232.89 (N–H), 3338.66 (N–H); ^{1}H NMR (400 MHz, DMSO-d_6) δ (ppm):3.13–3.19 (dd, 1H, pyrazoline CH_aH, $J = 5.6$ Hz, 18.0 Hz), 3.80–3.88 (dd, 1H, pyrazoline CHH_b, $J = 12.0$ Hz, 18.0 Hz), 5.34–5.38 (dd, 1H, pyrazoline CH_c, $J = 5.6$ Hz, 12.4 Hz), 7.08–7.20 (m, 2H, CH arom), 7.35–7.42 (m, 2H, CH arom), 7.50–7.51 (m, 3H, CH arom), 7.53–7.55 (d, 2H, CH arom, $J = 8.0$ Hz), 7.60–7.64 (m, 1H, CH arom), 7.83–7.85 (d, 2H, CH arom, $J = 7.6$ Hz), 7.88–7.90 (m, 2H, CH arom), 9.40 (s, 1H, NH_{2N}), 9.70 (s, 1H, NH_{1N}); ^{13}C NMR (100 MHz, DMSO-d_6) δ (ppm): 41.61, 59.75, 124.12, 125.33, 126.80, 127.42, 128.62, 130.07, 130.50, 131.01, 132.61, 133.07, 139.44, 144.88, 152.35, 152.84; Anal. Calcd for $C_{22}H_{19}ClN_4O_3S$: C, 58.08; H, 4.21; N, 12.32; S, 7.05. Found: C, 58.10; H, 4.25; N, 12.33; S, 7.10; ESI MS: $m/z =$ 454.93 $[M + H]^+$.

N'-*(benzenesulfonyl)-3,5-diphenyl-4,5-dihydro-1H-pyrazole-1-carbohydrazide* ***(2n)***

Light-yellow colored crystals. Yield: 69%; m.p. 230–231 °C; UV–Vis λ_{max} (nm): 295.41, 216.69; FTIR stretching frequencies (cm^{-1}): 1166.85 and 1331.97 (S=O), 1474.15 (C=N), 1690.43 (C=O), 3069.55 (Ar–H), 3211.68 (N–H), 3418.56 (N–H); ^{1}H NMR (400 MHz, DMSO-d_6) δ (ppm): 3.13–3.19 (dd, 1H, pyrazoline CH_aH, $J = 5.6$ Hz, 17.6 Hz), 3.83–3.91 (dd, 1H, pyrazoline CHH_b, $J = 12.0$ Hz, 18.0 Hz), 5.40–5.44 (dd, 1H, pyrazoline CH_c, $J = 5.6$ Hz, 12.0 Hz), 7.34–7.34 (d, 2H, CH arom, $J = 8.4$ Hz), 7.49–7.53 (m, 5H, CH arom), 7.56–7.60 (m, 1H, CH arom), 7.71–7.73 (d, 2H, CH arom, $J = 8.4$ Hz), 7.81–7.84 (d, 2H, CH arom, 7.2 Hz), 7.88–7.90 (m, 2H, CH arom), 9.43 (s, 1H, NH_{2N}), 9.60 (s, 1H, NH_{1N}); ^{13}C NMR (100 MHz, DMSO-d_6) δ (ppm): 41.43, 59.98, 125.46, 125.58, 126.31, 126.81, 127.51, 127.86, 128.59, 130.09, 130.97, 132.48, 139.31, 147.02, 152.31, 152.78; Anal. Calcd for $C_{22}H_{20}N_4O_3S$: C, 62.84; H, 4.75; N, 13.32; S, 7.62. Found: C, 62.80; H, 4.75; N, 13.30; S, 7.68; ESI MS: $m/z = 420.49$ $[M + H]^+$.

Biological assay

Antitubercular studies

Antitubercular activity was carried out against strain *M. tuberculosis* by MABA method (Franzblau et al. 1998).The outer perimeter wells of sterile 96-wells plate (falcon, 3072: Becton Dickinson, Lincoln Park NJ) was covered with 200 µL of sterile deionized water to minimize evaporation of the medium. The 96-wells plate received 100 µl of the Middlebrook 7H9 broth (Difco laboratories, Detroit, MI, USA) and serial dilutions of compounds were made directly on the plate. The final drug concentrations tested were 100 to 0.8 µg/mL. Plates were covered and sealed with parafilm and incubated at 37 °C for 5 days. After 5 days 25 µl of freshly prepared 1:1 mixture of almar blue reagent (Accumed International, Westlake Ohio) and 10% tween 80 was added to the plate and incubated for 24 h. A blue color in the well was interpreted as no bacterial growth and pink color was scored as growth. The results were compared with the MIC

of standard drug pyrazinamide, ciprofloxacin, and streptomycin.

Antimicrobial studies

The in vitro antimicrobial activity was done by disc diffusion method (Isenberg 2007). The compounds under the test were dissolved in analytically pure dimethylsulfoxide and geometric dilutions ranging from 75 to 5 µg/mL of the compounds. The test strains were spread on solid agar surface by using sterile swap. The turbidity was adjusted with broth to equal that of 0.5 Mc Farland standards. At the same time, absorbent paper discs were placed on agar surface and impregnated with a known concentration of stain and standard. The plates were inverted and allowed to incubate at 37 °C for about 24 h. The inhibition zone around the disc was calculated edge to edge zone of confluent growth, which was usually, corresponds to the sharpest edge of the zone and to be measured diameter in millimeter. The ciprofloxacin and fluconazole were used as a standard drug for antibacterial and antifungal activity, respectively.

Crystal structure

The X-ray intensity data were collected at the temperature of 293(2) K on a Bruker Proteum2 charge-coupled device diffractometer equipped with an X-ray generator operating at 45 kV and 10 mA, using CuKα radiation of wavelength 1.54178 Å. Data were collected for 24 frames per set with different settings of θ (0° and 90°), keeping the scan width of 0.5°, exposure time of 2 s, the sample to detector distance of 45.10 mm and 2è value at 46.6°. The complete data sets were processed using *SAINT PLUS* (Bruker 2012). The structures were solved by direct methods and refined by full-matrix least squares method on F^2 using *SHELXS* and *SHELXL* programs (Sheldrick 2008). The geometrical calculations were carried out using the program *PLATON* (Spek and Van der sluis 1990). The molecular and packing diagrams were generated using the software *MERCURY* (Macrae et al. 2008).

Acknowledgements We are thankful to Sigma-Aldrich Chemical Pvt. Ltd. Bengaluru, India, for providing necessary laboratory facilities for the research work and valuable support.

Compliance with ethical standards

Conflict of interest The authors declare that they have no competing interests.

References

Ahn JH, Kim HM, Jung SH, Kang SK, Kim KR, Rhee SD, Yang SD, Cheon HG, Kim SS (2004) Synthesis and DP-IV inhibition of cyano-pyrazoline derivatives as potent anti-diabetic agents. Bioorg Med Chem Lett 14:4461–4465

Ali MA, Siddiqui AA, Yar MS, Husain A, Abdullah M (2007) Synthesis and in-vitro antimycobacterial activity of amino-5 [(substituted)phenyl]-3-(4-hydroxy-3- methylphenyl]-4,5-dihydro-1*H*-1-pyrazolylmethanethione. Acta Pol Pharm 63:435–439

Balseven H, Isgor MM, Merta S, Alım Z, Beydemir S, Ok S, Kasımogullar R (2013) Facile synthesis and characterization of novel pyrazole-sulfonamides and their inhibition effects on human carbonic anhydrase isoenzymes. Bioorg Med Chem Lett 21:21–27

Bano S, Javed K, Ahmad S, Rathish IG, Singh S, Alam MS (2011) Synthesis and biological evaluation of some new 2-pyrazolines bearing benzenesulfonamide moiety as potential anti-inflammatory and anti-cancer agents. Eur J Med Chem 46:5763–5768

Bansal E, Srivatsava VK, Kumar A (2001) Synthesis and anti-inflammatory activity of 1- acetyl-5-substitutedaryl-3-β-aminonapthyl)-2-pyrazolines and β- (substitutediaminoethyl) amidonaphthalenes. Eur J Med Chem 36:81–92

Bashir R, Ovais S, Yaseen S, Hamid H, Alam MS, Samim M, Singh S, Javed K (2011) Synthesis of some new 1,3,5-trisubstituted pyrazolines bearing benzenesulfonamide as anticancer and anti-inflammatory agents. Bioorg Med Chem Lett 21:4301–4305

Bassindale A (1984) The third dimension in organic chemistry. Wiley-Blackwell, New York

Batulin YM (1968) Study of the effectiveness of cholinolytics as antidotes in poisoning with anticholinesterase compounds of mice and rats. Farmakol Toksikol 31:533–536

Bhat AR, Athar F, Azam A (2009) Bis-pyrazolines: Synthesis, characterization and antiamoebic activity as inhibitors of growth of *Entamoeba histolytica*. Eur J Med Chem 44:426–431

Bruker (2012) SAINT PLUS. Bruker AXS Inc. Madison

Chibale K, Haupt H, Kendrick H, Yardley V, Saravanamuthu A, Fairlamb AH, Croft SL (2001) Antiprotozoal and cytotoxicity evaluation of sulfonamide and urea analogues of quinacrine. Bioorg Med Chem Lett 11:2655–2657

Ezabadi IR, Camoutsis C, Zoumpoulakis P, Geronikaki A, Soković M, Glamočilija J, Čirič A (2008) Sulfonamide-1,2,4-triazole derivatives as antifungal and antibacterial agents: synthesis, biological evalution, lipophilicity and conformational studies. Bioorg Med Chem 16:1150–1161

Franzblau SG, Witzig RS, Mclaughlin JC, Torres P, Madico G, Hernandez A, Degnan MT, Cook MB, Quenzer VK, Ferguson RM, Gilman RH (1998) Rapid, low-technology MIC determination with clinical *mycobacterium tuberculosis* isolates by using the micro plate alamar blue assay. J Clin Microbiol 36:362–366

Gal CS (2001) An overview of SR121463, a selective non-peptide vasopressin V_2 receptor antagonist. Cardiovascular Drug Rev 19:201–214

Hassner A, Michelson MJ (1962) NMR spectra and stereoisomerism in pyrazolines. J Org Chem 27:3974–3976

Isenberg HD (2007) Clinical microbiology procedures handbook. American society for microbiology, Washington, DC

Kanda Y, Kawanishi Y, Oda K, Sakata T, Mihara S, Asakura K, Kanemasa T, Ninomiya M, Fujimoto M, Kanoike T (2001) Synthesis and structure-activity relationship of potent and orally active sulfonamide ET_B selective antagonists. Bioorg Med Chem 9:897–907

Kennedy JF, Thorley M (1999) Pharmaceutical Substances. 3rd ed. Thieme, Stuttgart, Germany

Macrae CF, Bruno IJ, Chisholm JA, Edgington PR, McCabe P, Pidcock E, Rodriguez-Monge L, Taylor R, van de Streek J, Wood PA (2008) *Mercury CSD 2.0* - new features for the visualization and investigation of crystal structures. J Appl Cryst 41:466–470

Natarajan A, Guo Y, Harbinski F, Fan YH, Chen H, Luus L, Diercks J, Aktas H, Chorev M, Halperin JA (2004) Novel arylsulfoanilide-oxindole hybrid as an anticancer agent that inhibits translation initiation. J Med Chem 47:4979–4982

Parmar SS, Pandey BR, Dwivedi C, Harbinson RD (1974) Anticonvulsant activity and monoamine oxidase inhibitory properties of 1,3,5-trisubstituted pyrazolines. J Pharm Sci 63:1152–1155

Prasad YR, Rao AL, Prasoona L, Murali K, Kumar PR (2005) Synthesis and antidepressant activity of some 1,3,5-triphenyl-2-pyrazolines and 3-(2"-hydroxy naphthalen-1"-yl)-1,5- diphenyl-2-pyrazolines. Bioorg Med Chem Lett 15:5030–5034

Raghav N, Singh M (2014) SAR studies of differently functionalized chalcones based hydrazones and their cyclized derivatives as inhibitors of mammalian cathepsin B and cathepsin H. Bioorg Med Chem 22:4233–4245

Sammes PG (1990) The rational design, mechanistic study and therapeutic application of chemical compounds, Chapter 7.1, In: Hansch C, Sammes PG, Taylor JB (ed), Comprehensive medicinal chemistry, Vol 2. Pergamon Press, Oxford, UK

Shaharyar M, Siddiqui AA, Ali MA (2006) Synthesis and evaluation of phenoxy acetic acid derivatives as a anti-mycobacterial agents. Bioorg Med Chem Lett 16:4571–4574

Sheat MA, Sultan AH, Farage AM (2011) Synthesis of some aryl sulfonamide compounds from o-nitrotoluene. Raf J Sci 22:57–61

Sheldrick GM (2008) A short history of *SHELX*. Acta Cryst A64:112–122

Siddiqui ZN, Musthafa TNM, Ahmad A, Khan AU (2011) Thermal solvent-free synthesis of novel pyrazolyl chalcones and pyrazolines as potential antimicrobial agents. Bioorg Med Chem Lett 21:2860–2865

Soni N, Pande K, Kalsi R, Gupta TK, Parmar SS, Barthwal JP (1987) Inhibition of rat brain monoamine oxidase and succinic dehydrogenase by anticonvulsant pyrazolines. Res Commun Chem Pathol Pharmacol 56:129–132

Spek AL, Van der sluis P (1990) Bypass: an effective method for the refinement of crystal structures containing disordered solvent regions. Acta Cryst A46:194–201

Stokes SS, Albert R, Buurman ET, Andrews B, Shapiro AB, Green OM, McKenzie AR, Otterbein LR (2012) Inhibitors of the acetyltransferase domain of N- acetylglucosamine-1-phosphate-uridylyltransferase/glucosamine-1-phosphate- acetyltransferase (GlmU). Part 2: optimization of physical properties leading to antibacterial aryl sulfonamides. Bioorg Med Chem Lett 22:7019–7023

Stuart BH (2004) INFRARED SPECTROSCOPY: fundamentals and applications. Wiley, West Sussex, England

Sverdlova OV, Korzhikova LM, Ioffe BV (1968) Near –UV absorption spectra of pyrazolines. J Appl Spectrosc 8:77–79

Turan-Zitouni G, Chevallet P, Kilic FS, Erol K (2000) Synthesis of some thiazolyl-pyrazoilne derivatives and preliminary investigation of their hypotensive activity. Eur J Med Chem 35:635–641

Wang SQ, Wu QH, Wang HY, Zheng XX, Shen SL, Zhang YR, Miao JY, Zhao BX (2013) A novel pyrazoline-based selective fluorescent probe for detecting reduced glutathione and its application in living cells and serum. Analyst 138:7169–7174

WHO (2014) Global tuberculosis report. Geneva

Wu J, Zhang D, Chen L, Li J, Wang J, Ning C, Yu N, Zhao F, Chen D, Chen X, Chen K, Jiang H, Liu H, Liu D (2013) Discovery and mechanism study of SIRT1 activators that promote the deacetylation of fluorophore-labeled substrate. J Med Chem 56:761–780